RESEARCH PAPER

PCCP
www.rsc.org/pccp

Size mismatch effects in oxide solid solutions using Monte Carlo and configurational averaging

Chris E. Mohn,[a] Mikhail Yu. Lavrentiev,†[b] Neil L. Allan,[b] Egil Bakken‡[a] and Svein Stølen[a]

[a] *Department of Chemistry, University of Oslo, Postbox 1033 Blindern, N0315 Oslo, Norway. E-mail: svein.stolen@kjemi.uio.no*
[b] *University of Bristol, School of Chemistry, Cantock's Close, BS8 1TS Bristol, England*

Received 4th October 2004, Accepted 10th January 2005
First published as an Advance Article on the web 11th February 2005

Local minima configurational averaging (CA) and Monte Carlo (MC) simulations are used to examine in detail the variation of thermodynamic and structural properties of binary oxide solid solutions with the volume mismatch between the end members. The maximum volume mismatch studied corresponds to that in the CaO–MgO solid solution, a prototype example of a strongly non-ideal system with large miscibility gap. In addition, solid solutions of CaO–HypO using designed hypothetical atoms (Hyp) with atomic radii between those of Ca^{2+} and Mg^{2+} have been considered. Calculations on the hypothetical systems allow not only the systematic investigation of size mismatch, but also the detailed examination and comparison of the CA and MC methods. A particularly efficient implementation of the CA method is *via* the rapid calculation of the radial distribution function (RDF) for all possible arrangements obtained by distributing the different ions on their respective crystallographic sites followed by full structural optimisation of just one configuration from each group with the same RDF. Comparison of results from CA, using optimisations in the static limit, and MC indicates the importance of cell-size and vibrational effects, which can be particularly important for the largest size mismatches. The enthalpies, excess configurational entropies, vibrational entropies and volumes of mixing scale roughly quadratically for all but the largest volume mismatches. Equally sized atoms cluster together in the first coordination shell for all volume mismatches studied.

1. Introduction

Traditionally, ordered compounds have received more attention in solid-state chemistry than disordered systems. Disorder has been difficult to characterise both structurally and computationally. While structural studies of disordered materials until recently have been carried out on quenched samples mainly, the vast majority of theoretical studies have focused on periodic ordered systems. During recent years more effort has been made to characterise disordered materials experimentally through *in situ* high temperature studies and also computationally using semiclassical atomistic simulations or more elaborate *ab initio* quantum mechanical methods.

The approach taken here for studying disordered systems is based on two multiconfigurational techniques Monte Carlo and configurational averaging, in which a large number of atomic arrangements are considered within the constraints imposed by periodic boundary conditions. These arrangements are thought of as representing possible local structural features of the real disordered material. In previous work configurational averaging was used to denote full Gibbs energy minimizations using lattice statics and lattice dynamics followed by thermodynamic averaging of the energies of the resulting local minima, and has provided a useful tool for the calculation of various properties of disordered solids over a broad range of temperatures and pressures.[1–3] For example, calculated values of the enthalpy of mixing for a solid solution of MgO and MnO using CA with a supercell of 256 atoms and only 250 randomly chosen configurations, were in very good agreement with results obtained from Monte Carlo, and also with correlation-corrected *ab initio* Hartree–Fock (HF) calculations.[4] The resulting miscibility gap reported in ref. 1 was in good agreement with that obtained experimentally by Wood *et al.*,[5] suggesting complete solid solubility above 1100 K. Hybrid methods, which combine either MC and molecular dynamics[1] or MC and energy minimisation techniques,[6] have been shown to be powerful tools for the investigation of disordered systems with small and modest size mismatch between the end-members. Examples are investigations of the phase transition in solid solutions of $MgSiO_3$ and $MnSiO_3$ perovskites[1] and structural features of Al–Fe disorder in $Ca_2Fe_xAl_{2-x}O_5$ brownmillerite-type perovskites.[6,7]

Solid solutions of binary oxides with large volume mismatch have also been studied by a number of different theoretical approaches. Calculations of the enthalpy of mixing for solid solutions of CaO and MgO has been studied using either DFT or different sets of pair potentials. In addition, results from multiconfigurational or single configurational techniques with or without including vibrational contributions have been reported. The enthalpies of mixing calculated using density functional theory in conjunction with multiple scattering theory[8] are in qualitative agreement with those obtained from Monte Carlo simulations,[1,9] but significantly larger than the self-consistent potential induced breathing (SCPIB) results reported in[10] which considered only a few ordered arrangements. By contrast, the enthalpies of mixing obtained using pair potentials reported in the same article[10] were, in general significanly larger than the results reported in refs. 1, 8 and 9. Two different approaches have also been used to calculate the solid-solubility limits. The phase-diagram of CaO–MgO calculated using exchange MC techniques[9] and pair potentials is in

† On leave from the Institute of Inorganic Chemistry, 630090 Novosibirsk, Russia.
‡ Present address: Norwegian Defence Research Establishment, Postbox 25, N2027 Kjeller, Norway.

DOI: 10.1039/b415340e

qualitatively good agreement with experiment,[11] the solid-solid solubility limits are however significantly smaller than those obtained experimentally. The calculated miscibility gap for CaO–MgO obtained using the SCPIB model[10] was in good agreement with experiment. Thus systems involving large volume mismatch such as solid solutions of MgO and CaO continue to present challenges to the theoretician.

Davies and Navrotsky[12] have systematically studied volume mismatch effects in various binary solid solutions. By fitting the regular solid solution model to available solubility and activity–composition data for a wide variety of structure types and plotting the resulting Gibbs energy parameter *vs.* a term describing the volume mismatch between the end members, they proposed a linear correlation, although there is considerable spread in the data. A regular solid solution model was in addition used to fit available calorimetric enthalpy data. In these cases, a much better correlation between the resulting enthalpy parameter and the volume mismatch was obtained for alkali halides. However, it was not clear from the available experimental data whether this enthalpy parameter varied linearly or quadratically with the volume mismatch between the end members. Also for binary oxide solid solutions the enthalpy parameter was found to increase as the volume mismatch increases. However, in contrast to what they observed for alkali halides the increase was somewhat irregular, most likely due to the possible influence of electronic effects in some systems involving transition metal ions (*e.g.*, NiO–MgO).

The volume mismatches studied here include the solid solution of CaO and MgO, a prototype example of a strongly non-ideal system with large size mismatch, and solid solutions of CaO–HypO using designed hypothetical ions (Hyp) with ionic radii between those of Ca^{2+} and Mg^{2+}. A major advantage of atomistic simulations using empirical potentials is that one is able to *mix* potentials for different materials to construct *new* hypothetical systems. For instance, by interpolating potential parameters reported for MgO and CaO one can create a new *hypothetical* binary oxide, HypO. First, the binary oxide HypO potentials are constructed using an appropriate scheme and then various properties for CaO–HypO are calculated using a large number of different local minima configurations. A similar approach has been taken by Bosenick *et al.*[13] who used potentials for hypothetical oxides to study systematically scaling of thermodynamic mixing properties in garnet solid solutions.[13]

In this paper we pay particular attention to the CA method for the study of the scaling of thermodynamic properties of binary oxide solid solutions. This involves *full* structural optimisations of a large number of different configurations. The rapid growth of the number of different arrangements when increasing the size of the supercell inherently limits the applications of the CA, and hence techniques for selecting a small number of representable configurations are highly desirable. In systems with a large degree of short range order, where the interacting species tend to produce a few low-energy configurations, taking a small number of randomly chosen configurations may fail to sample adequately the disordered state. In this paper we show how the rapid calculation of the radial distribution function (RDF)[14] provides a computationally efficient tool for selecting a small number of configurations to optimise as well as calculation of the associated weightings, which enables us to compute the enthalpy, entropy, Gibbs energy and volume of mixing including billions of possible distributions of cations. Calculations on the hypothetical systems we have chosen allow us not only to investigate the size mismatch effects systematically but also to examine in detail the CA and RDF methods. We also compare with results from Monte Carlo simulations, in particular to assess the importance of cell-size effects and contributions from lattice vibrations.

This paper is organised as follows: In section 2 we describe how averaged properties can be calculated using statistical thermodynamics, the RDF method is introduced, and the MC method is also presented. Thereafter, three different *schemes* for constructing potentials for hypothetical oxides are described. In section 3, results from test calculations using these three different schemes for constructing hypothetical potentials are presented, and the results from the RDF approach is compared with that based on random selection of configurations to optimise. CA and MC simulations are compared, effects of cation size mismatch on the immiscibility of the oxides are examined and the scaling of various thermodynamic and structural properties with the volume mismatch between the end-members is discussed. We conclude in section 4.

2. Theory and computational details

2.1. Thermodynamic properties: Configurational averaging and the RDF method

For calculations of thermodynamic and structural properties for disordered systems, we assume the existence of $\binom{N}{n}$ local minima on the potential energy surface corresponding to $\binom{N}{n}$ *initial* configurations obtained by distributing the cations on the crystallographic cation sites of the NaCl-type structure. Here, N is the total number of cations, and n the number of minority cations. From all the $\binom{N}{n}$ *relaxed* arrangements the thermodynamic properties are calculated using statistical thermodynamics as described elsewhere.[15] Equations for the enthalpy, Gibbs energy and entropy in the NPT ensemble are given by:

$$H = \frac{\sum_k H_k \exp(-G_k/k_B T)}{\sum_k \exp(-G_k/k_B T)},$$

$$G = -k_B T \ln \sum_k \exp\left(\frac{-G_k}{k_B T}\right), \qquad (2.1)$$

$$S = \frac{H}{T} + k_B \ln \sum_k \exp\left(\frac{-G_k}{k_B T}\right),$$

where G_k is the Gibbs energy for the relaxed structure of arrangement k, and k runs over all $\binom{N}{n}$ configurations. Other properties, Y, such as averaged volumes can be calculated using an expression analogous to that for the enthalpy:

$$Y = \frac{\sum_k Y_k \exp(-G_k/k_B T)}{\sum_k \exp(-G_k/k_B T)} \qquad (2.2)$$

All optimisations are carried out in the static limit so that $G_k = H_k$. k_B is Boltzmann's constant. In this paper we introduce two cluster parameters γ_1 and γ_2 which are also calculated using eqn. (2.2). We define γ_1 and γ_2 as the number of hypothetical cations in the nearest and second-nearest coordination-sphere, respectively, around a hypothetical atom divided by the values expected if the two types of cation in the solid solution were randomly distributed. Values of γ_1 and γ_2 larger than one indicate that the same type of cation tends to cluster in the first or second coordination shell, respectively.

With the exception of the smallest cells, the optimisation of *all* $\binom{N}{n}$ initial configurations is a horrendously time-consuming task, and other approaches are required. In one of these, a fraction of the total number of initial arrangements are selected at random and optimised, and the summations in eqns. (2.1) and (2.2) are restricted to a fraction of the total number of arrangements. In the thermodynamic average they are all given equal weight. However, a random selection of configurations may fail to sample the disordered state where only a small

fraction are thermally accessible such as in strongly non-ideal systems and, in general, in disordered materials at low temperature. We have therefore developed a new technique based on the rapid computation of the radial distribution functions,[14] and making the approximation that configurations with the same RDF have the same minimised Gibbs energy G_k. *All* possible distributions of a given composition and supercell are calculated and one initial configuration from each unique RDF is selected at random and optimised. The number of configurations to optimise is simply the number of non-equivalent RDFs. In the thermodynamic average each optimised configuration is weighted by the number of initial configurations with the *same* RDF. The RDF approach is powerful in the sense that it involves a rapid comparison routine in order to select configurations to optimise; billions of RDFs can be calculated within a few CPU-hours, using modern massively parallel computers. We refer to this technique as RDF(full) where *full* means that RDFs are calculated for all $\binom{N}{n}$ configurations. The RDF(full) method currently scales quadratically with system size, and techniques in order to allow for linear scaling are under development. Once the RDFs are calculated for a given crystal system with a given composition, it can be applied to all compounds with that structure and composition. It is worth emphasising that configurations with the same RDF do not necessarily have the same *relaxed* energies, and therefore an error is introduced because configurations with the same RDFs *may* relax differently.

For the static optimisations of the individual initial configurations of HypO and CaO solid solutions we have used the program package GULP.[16] Optimisation of all unit cell dimensions and atomic coordinates was carried out in the static limit ($T = 0$ K and in the absence of lattice vibrations). No symmetry constraints are applied during the structural optimisations.

We have chosen a modest sized 64-atom supercell for calculations of thermodynamic and structural properties of CaO and HypO solid solutions in which the conventional eight-ion cubic cell is doubled along each axis. This cell provides a wide range of possible arrangements and related calculations on MgO–MnO solid solutions show that reliable thermodynamic properties are obtained at low computational cost.[3] Results from test calculations using a 96 atom cell with composition $X_{\mathrm{HypO}} = 0.125$ are also reported in which the conventional cell was trebled along one of the axis and doubled along the other two axis. In this case, 12 million configurations reduces to 8131 RDF-non-equivalent configurations.

For calculations of the averaged cluster-parameters γ_1 and γ_2 involving cations with large size mismatch, cutoffs for the relevant coordination-spheres must be assigned carefully. Usually, the cut-off chosen for the first coordination-sphere is the mean of typical distances for cation–cation nearest and cation–cation next-nearest neighbours. Similarly, the upper cut-off for the second coordination sphere is the mean of distances for cation–cation next-nearest neighbour and cation–cation third-nearest neighbours. When the size mismatch is large it is not straightforward to define unique thresholds for different coordination spheres because there are relaxed configurations that contain cation–cation second-nearest neighbour distances that are smaller than cation–cation nearest neighbour distances in some other relaxed configurations. A given cut-off for *e.g.* the first coordination sphere is therefore not able to include all cation–cation nearest neighbour distances for all the configurations and at the same time exclude all second-nearest neighbour distances. In these cases γ_1 and γ_2 are sensitive to changes in the cutoff distances, and the selection of thresholds for the different coordination spheres was based on inspection of distances for a large number of configurations. For solid solutions of MgO and HypO with 7, 14, 23 and 30% volume mismatch between the binary oxides, the cutoffs for the first and second coordinations spheres were 4.2 Å and 5.2 Å, respectively. The same cutoffs (4.2 Å and 5.2 Å, respectively for the first and second coordination sphere) were used for solid solution of CaO and MgO (39% volume mismatch) with composition $X_{\mathrm{HypO}} = 0.125$. For solid solutions of CaO and MgO with composition $X_{\mathrm{HypO}} = 0.5$ the upper thresholds of the radii of coordination spheres were 3.85 Å and 5.15 Å for the first and second coordination shells, respectively.

2.2. MC simulations

The Monte Carlo simulations presented in this work are carried out in the *NPT* ensemble using the Monte Carlo exchange (MCX) technique in which both the atomic configuration and the atomic coordinates of all the atoms are changed.[9] In any step, a random choice is made whether to attempt a random exchange between two cations, a random displacement of an ion, or a random change in the volume of the simulation box. The step is either accepted or rejected using the usual Metropolis algorithm.[17] Most simulations here use a box-size of 512 ions and 5×10^7 steps in the production stage, following initial equilibration of 1×10^7 steps. The maximum changes in the atomic displacements and the lattice parameters are governed by the variables $r_{\max}$ and $v_{\max}$ respectively. The magnitudes of these parameters are adjusted automatically during the equilibration part of the simulation to maintain an acceptance/rejection ratio of approximately 0.3.

In addition to random movements of atoms, or cell volume we also make an exchange of two cations chosen at random again with the acceptance/rejection decision made using the Metropolis scheme. In the systems studied in this paper, the efficiency of this exchange may be very low due to the large difference in ionic radii and potential parameters. Low exchange rate slows the equilibration, so that special methods are necessary to increase the rate of successful exchanges. To speed up the sampling of configurations we have applied configurational-bias Monte Carlo.[9] Here, instead of considering a single trial exchange, a set of trial exchanges is picked at random. Suppose an exchange take place between atoms A and B. First, k pairs $\{A^i, B^i, i = 1,\ldots,k\}$ are randomly chosen. We denote the system potential energy in the initial configuration as ϕ_{old} and the energy of the system after exchange of atoms in the ith pair as ϕ^i_{new}. One of the new configurations is then chosen with probability

$$p_i = \frac{\exp(-\beta(\phi^i_{\mathrm{new}} - \phi_{\mathrm{old}}))}{W_{\mathrm{new}}} \tag{2.3}$$

where $\beta = (k_{\mathrm{B}}T)^{-1}$ and

$$W_{\mathrm{new}} = \sum_{i=1}^{k-1} \exp(-\beta(\phi^i_{\mathrm{new}} - \phi_{\mathrm{old}})). \tag{2.4}$$

The chosen configuration i (that after the exchange of the ith pair) with energy $\phi^i_{\mathrm{new}} \equiv \phi_{\mathrm{new}}$ is then the trial configuration. However, the usual acceptance rule[17] cannot be directly applied. Instead, starting from the new configuration, a further $k - 1$ pairs are chosen $\{A^j, B^j, j = 1,\ldots,k-1\}$. Denoting the energy of the system after exchange of atoms in the jth pair $\phi^{\mathrm{j}}_{\mathrm{old}}$, we evaluate the expression

$$W_{\mathrm{old}} = \exp(-\beta(\phi_{\mathrm{old}} - \phi_{\mathrm{new}})) + \sum_{j=1}^{k-1} \exp(-\beta(\phi^j_{\mathrm{old}} - \phi_{\mathrm{new}})). \tag{2.5}$$

Fulfilling detailed balance, the criterion for the acceptance of the new configuration is

$$\min[1, \exp(-\beta(\phi_{\mathrm{old}} - \phi_{\mathrm{new}}))W_{\mathrm{new}}/W_{\mathrm{old}}] \tag{2.6}$$

Use of the exchange-bias technique with $k = 100$ makes possible Monte Carlo simulations with a successful exchange rate of Ca^{2+} and hypothetical cations of between 10% and 70% at 1000 K, depending on hypothetical ion size. We have checked that this is sufficient for convergence of the properties of interest for this paper.

The semi-grand-canonical ensemble method has been used in conjunction with the Monte Carlo calculations to calculate the difference in chemical potential between cations, and hence the excess Gibbs energy and the entropy.[9,18] In this method one species, B, is converted into another, A, and the resulting potential energy change $\Delta\phi_{B/A}$ determined. This is related to the change in chemical potential $\Delta\mu_{B/A}$ by

$$\Delta\mu_{B/A} = -\frac{1}{\beta}\ln\left\langle \frac{N_B}{N_A + 1}\exp(-\Delta\phi_{B/A}\beta)\right\rangle. \qquad (2.7)$$

Each fifth step (on average) we evaluate the energy associated with the conversion of a randomly chosen hypothetical ion to Ca^{2+}, $\Delta\phi_{Hyp/Ca}$, and as the simulation proceeds determine the average value of the right hand side of eqn. (2.5). Note that the change of Hyp into Ca is only considered but not actually performed – the configuration remains unchanged after evaluating $\Delta\phi_{Hyp/Ca}$. We have checked consistency in that, overall, identical results are obtained considering the reverse transformation, *i.e.*, of a randomly chosen Ca to a Hyp. Given the values of $\Delta\mu_{B/A}$, values of $\Delta_{mix}G$ and $\Delta_{mix}S$ (*via* $\Delta_{mix}G = \Delta_{mix}H - T\Delta_{mix}S$) are obtained as described in ref. 9. Most Monte Carlo results presented here use a simulation cell containing 512 atoms, and we have checked the convergence of the Monte Carlo results with simulation cell size.

2.3. Potentials for hypothetical oxides

All simulations in this study are based on the Born model using an Ewald sum to evaluate long-range Coulombic forces, while the short-range electron-electron repulsion and Van der Waals interactions are modelled by a Buckingham pair potential:

$$V(r) = A\exp\left(\frac{-r}{\rho}\right) - \frac{C}{r^6}. \qquad (2.8)$$

r is the inter-ionic distance, and the parameters, A, ρ and C are fixed for a given interaction. A conventional Born model is used, assigning integral ionic charges (2+) to Ca, Mg and the hypothetical atoms. In the CA calculations, ionic polarisability of the O^{2-} ions is treated using the shell model of Dick and Overhauser.[19] Test calculations using different potential parameters reported in the literature[4,10,20,21] were carried out. The widely used potential parameters for MgO and CaO developed by Lewis and Catlow[21] were found to be the most suitable for our purposes and were used in this study.

For the construction of potentials for hypothetical oxides three different schemes are considered. We will refer to these schemes as the fitted-function, the linear and the Winkler scheme. We have plotted the potential parameters representing the hypothetical oxides for the different schemes in Fig. 1.

In the *fitted function scheme* we assume that we can interpolate the potentials reported for MgO, CaO and SrO, by fitting some smooth function.

In the strategy proposed by Winkler *et al.*,[22] the hypothetical potentials are constructed using the condition that the first and second derivatives with respect to the inter-ionic distance r of the hypothetical potential should be equal to the stoichiometric sum of derivatives for the potentials of the constituent oxides

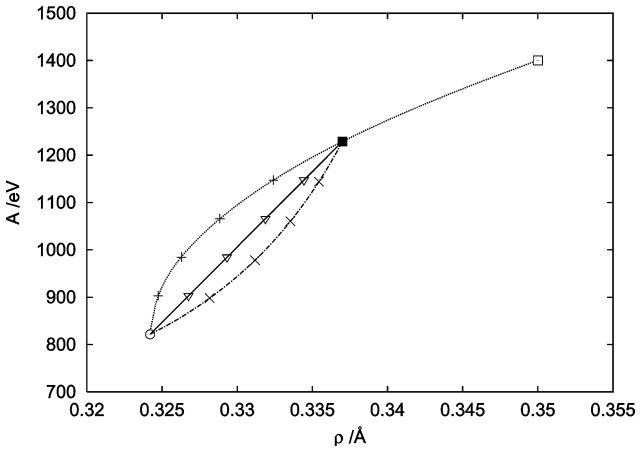

Fig. 1 The potential parameters representing hypothetical oxides constructed using Lewis and Catlow potentials for CaO, MgO and SrO (fitted function scheme only)[21] utilising the three different schemes described in the text. The open circle, full square and open square are used to represent the potentials for MgO, CaO and SrO respectively. Full, dotted and dashed-dotted lines are used to represent the interpolations of the linear scheme, the fitted function scheme and the Winkler scheme, respectively. The following symbols represent the potentials used in this study: + (fitted function scheme), × (Winkler scheme) and ▽ (linear scheme).

at the average atomic distance:

$$\rho_{Hyp_{(\chi)}O} = \begin{pmatrix} (1-\chi_{MgO})\rho_{CaO}^{-1}A_{CaO}\exp(-r_0/\rho_{CaO}) \\ +\chi_{MgO}\rho_{MgO}^{-1}A_{MgO}\exp(-r_0/\rho_{MgO}) \end{pmatrix} \times \begin{pmatrix} (1-\chi_{MgO})\rho_{CaO}^{-2}A_{CaO}\exp(-r_0/\rho_{CaO}) \\ +\chi_{MgO}\rho_{MgO}^{-2}A_{MgO}\exp(-r_0/\rho_{MgO}) \end{pmatrix}^{-1},$$

$$A_{Hyp_{(\chi)}O} = \begin{pmatrix} (1-\chi_{MgO})\rho_{CaO}^{-1}A_{CaO}\exp(-r_0/\rho_{CaO}) \\ +\chi_{MgO}\rho_{MgO}^{-1}A_{MgO}\exp(-r_0/\rho_{MgO}) \end{pmatrix} \times \left[\rho_{Hyp_{(\chi)}O}^{-1}\exp\left(-r_0/\rho_{Hyp_{(\chi)}O}\right)\right]^{-1}. \qquad (2.9)$$

Here r_0 is the arithmetic mean of the Ca–O and Mg–O distances in CaO and MgO, respectively (2.3 Å). χ varies from 0 to 1; when χ is 0 we regain the parent potential for CaO, and when χ is 1, the parent MgO potential.

Comparing the fitted function method and the Winkler scheme (see Fig. 1), the different paths taken in the parameter space on increasing χ suggest that other schemes are possible which yield potential parameters lying between the boundaries of those given by the fitted function scheme and the Winkler scheme. A very simple and intuitive approach is a *linear scheme* where the potential parameters representing hypothetical oxides are constructed using a simple linear interpolation:

$$A_{Hyp_{(\chi)}O} = A_{CaO} + \chi_{MgO}(A_{MgO} - A_{CaO}),$$
$$\rho_{Hyp_{(\chi)}O} = \rho_{CaO} + \chi_{MgO}(\rho_{MgO} - \rho_{CaO}). \qquad (2.10)$$

We define the volume mismatch as the absolute value of the differences between the calculated volumes (of CaO and HypO) divided by the mean of the volumes. In the three above-mentioned schemes the five potential parameters chosen representing hypothetical oxides resulted in roughly 39%, 30%, 23%, 14% and 7% volume mismatch, respectively, between CaO and HypO, the first of these being the volume mismatch between CaO and MgO. An advantage of the *linear* or *fitted function* schemes over that of the Winkler scheme is that no

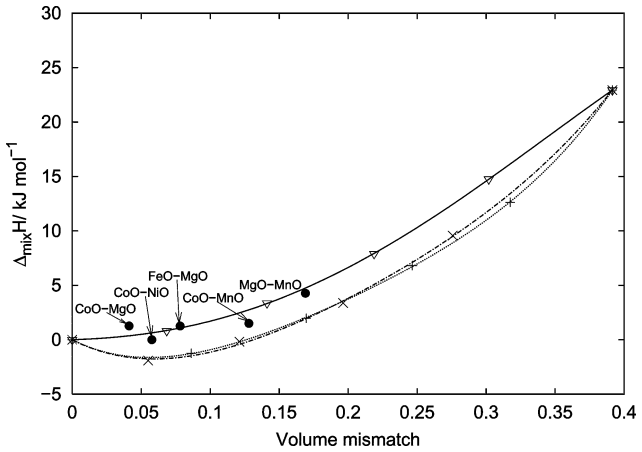

Fig. 2 Calculated $\Delta_{mix}H$ *vs.* the volume mismatch between the end members utilising the three different schemes for constructing potentials representing hypothetical oxides for a solid solution of CaO and HypO with composition $X_{HypO} = 0.5$. The following symbols were used for the different schemes: + (Fitted function scheme), × (Winkler scheme) and ▽ (The linear scheme). Full circles represent enthalpy parameters for a set of binary oxides solid solutions obtained by fitting a regular solid solution model to available experimental enthalpy of mixing data.[12]

a priori prediction of equilibrium bond distances is necessary in order to establish the potentials representing the hypothetical oxides. Nevertheless, it has been shown that the potentials for the hypothetical oxides are not sensitive to changes in the averaged cation–oxygen bond distance.[22] We stress that construction of potentials representing hypothetical oxides should be done in a systematic manner; A and ρ are highly correlated, and should not be changed independently. For a given set of hypothetical potential parameters the energy should converge both smoothly and quickly. Secondly a given set of hypothetical potential parameters should give rise to physically reasonable thermodynamic and structural properties.

3. Results and discussion

3.1. Schemes for constructing potentials for hypothetical oxides

Configurational averaged enthalpies of mixing *vs.* volume mismatch at 1000 K utilising the three different schemes for constructing potentials representing hypothetical oxides are shown in Fig. 2. Calculations were performed for solid solutions of the hypothetical oxides and CaO with composition $X_{HypO} = 0.5$. Selection of configurations and calculation of the associated weightings were carried out using the RDF(full) method which is discussed more fully in the next section.

We have also plotted $\Delta_{mix}H$ for a selection of binary oxide solid solutions using the enthalpy parameter obtained by fitting a regular solution model to available enthalpy of mixing data. The enthalpy of mixing data is insensitive to changes in the temperature. Thus, the difference in the temperature of the experiment and that used in the simulations has no significant effect when comparing with experimental results. The variation of $\Delta_{mix}H$ obtained using the linear technique is different from that obtained using the fitted function and the Winkler schemes. For all volume mismatches the enthalpies of mixing are positive using the linear schemes, in good agreement with available $\Delta_{mix}H$ obtained experimentally for binary-oxide solid solutions with comparable volume mismatches. In contrast, the forms of the potentials from the fitted function and the Winkler scheme give rise to an unphysical negative deviation from ideality for small mismatches. We have therefore used the linear scheme in the rest of this paper. Note that NiO–MgO is the only known rock salt system to exhibit negative deviation from ideality. This is however probably due to electronic effects.[12]

3.2. Configurational averaging: The RDF technique

Averaged thermodynamic and structural properties at 1000 K using configurational averaging with the RDF(full) approach and sets of randomly chosen configurations are listed in Table 1. Solid solutions of CaO and HypO with compositions $X_{HypO} = 0.125$ and $X_{HypO} = 0.5$ were chosen. The first case ($X_{HypO} = 0.125$) represents an important benchmark system since we are able to optimise all 35 960 possible arrangements and so assess the accuracy of methods in which not all configurations are chosen. 35 960 configurations reduces to 45 RDF-non-equivalent configurations for $X_{HypO} = 0.125$. When $X_{HypO} = 0.5$ it is not feasible to optimise all 600 million configurations. The RDFs are nevertheless quickly computed. 2656 RDF-non-equivalent configurations were found among the 601 080 390 configurations. The standard deviation reported are based upon results from ten different sets, where in each case, the configurations are randomly selected from different RDFs. The differences reflect the failure of the RDF approach to distinguish between symmetrically non-equivalent configurations with equal RDFs. Results using ten sets of 45 and 2656 randomly chosen configurations out of 35 960 and 600 million configurations, respectively, are also given (under RAND) in the table. The randomly chosen configurations were given equal weight.

First, we discuss solid solutions of CaO and HypO with composition $X_{HypO} = 0.125$. The standard deviations reported for thermodynamic properties using only 45 randomly chosen configurations out of totally 35 960 configurations are small for all volume mismatches considered. These findings are consistent with extensive studies of the MnO–MgO solid solution[1,3] where only a small fraction of the total number of configurations was sufficient for a wide range of thermodynamic properties. On the other hand, the somewhat larger standard deviations reported for the structural parameters, γ_1 and γ_2 suggest that a larger number of configurations is necessary in order to describe correctly clustering phenomena in these solid solutions with NaCl-type structure. For a set of 45 randomly chosen configurations, the standard deviations are too large to establish any tendency of equally sized atoms to cluster within the first coordination sphere.

Turning to the RDF(full) method ($X_{HypO} = 0.125$), the small standard deviations reported for the calculated thermodynamic and structural properties even when the volume mismatch is large is encouraging and emphasises that the RDF(full) method provide accurate thermodynamic and structural properties. The advantages of using the RDF(full) method over that of selecting configurations at random are greater when the volume mismatch is less than 30%. In these cases, the standard deviation reported for $\Delta_{mix}H$ using RDFs are typically one order of magnitude smaller than those introduced when configurations are randomly selected and weighted equally. When the volume mismatch is large (MgO–CaO), the energy-gap between RDF-equivalent configurations with different symmetries also increases. Hence in this case the sizes of the standard deviation reported using the RDF(full) method are only a factor of two smaller than those achieved using the random approach. For the structural parameters where 45 randomly chosen configurations fail to describe clustering-phenomena, the RDF(full) method is far superior. When the size mismatch is less than approximately 15% the standard deviations reported for γ_1 and γ_2 using the RDF(full) method are typically between two and three orders of magnitude smaller than those obtained using the approach where configurations are randomly selected and weighted equally. The results achieved using the RDF(full) method are sufficiently accurate to describe the increased clustering of equally sized

Table 1 Calculated averaged structural and thermodynamic properties using the RDF(full)- method for solid solutions of HypO and CaO at 1000 K with compositions $X_{HypO} = 0.125$ and $X_{HypO} = 0.5$. Results obtained using sets of randomly chosen configurations (RAND) given equal weight are also reported for comparison. For $X_{HypO} = 0.125$ and $X_{HypO} = 0.5$, 45 and 2656 RDF non-equivalent configurations, respectively, were selected randomly and optimised. In the RAND calculations for $X_{HypO} = 0.125$ and $X_{HypO} = 0.5$, 45 and 2656 configurations, respectively, were randomly selected, optimised and weighted equally

X_{HypO}	Method	Volume mismatch	$\Delta_{mix}H$/kJ mol^{-1}	$\Delta_{mix}G$/kJ mol^{-1}	$\Delta_{mix}S$/J K^{-1} mol^{-1}	γ_1	γ_2	$\Delta_{mix}V$/Å^3
0.125	RDF	0.0685	0.3566 ± 0.0001	−2.3685 ± 0.0001	2.7251 ± 0.0000	1.0092 ± 0.0001	0.9467 ± 0.0002	0.0012 ± 0.0000
		0.1412	1.4737 ± 0.0006	−1.2448 ± 0.0006	2.7185 ± 0.0001	1.0314 ± 0.0008	0.8258 ± 0.0019	0.0045 ± 0.0000
		0.2188	3.4614 ± 0.0026	0.7627 ± 0.0023	2.6987 ± 0.0008	1.0610 ± 0.0033	0.6985 ± 0.0076	0.0100 ± 0.0001
		0.3019	6.4660 ± 0.0085	3.8025 ± 0.0064	2.6635 ± 0.0036	1.1093 ± 0.0103	0.6052 ± 0.0198	0.0194 ± 0.0012
		0.3915	10.5778 ± 0.0724	7.9807 ± 0.0496	2.5971 ± 0.0258	1.2856 ± 0.0997	0.7197 ± 0.2186	0.0737 ± 0.0178
	RAND	0.0685	0.3576 ± 0.0042	−2.3675 ± 0.0044	2.7251 ± 0.0003	1.0456 ± 0.1822	0.5711 ± 0.2619	0.0013 ± 0.0002
		0.1412	1.4702 ± 0.0227	−1.2492 ± 0.0256	2.7194 ± 0.0040	1.0191 ± 0.0529	0.4657 ± 0.2930	0.0044 ± 0.0014
		0.2188	3.4586 ± 0.0364	0.7610 ± 0.0409	2.6976 ± 0.0079	1.0054 ± 0.1542	0.3964 ± 0.1843	0.0094 ± 0.0017
		0.3019	6.4567 ± 0.0792	3.8017 ± 0.0879	2.6550 ± 0.0437	1.1159 ± 0.2033	0.2033 ± 0.0454	0.0192 ± 0.0028
		0.3915	10.5639 ± 0.1593	7.9669 ± 0.1366	2.5970 ± 0.0437	1.3045 ± 0.3197	0.4349 ± 0.2430	0.0791 ± 0.0258
0.5	RDF	0.0685	0.8277 ± 0.0001	−4.4198 ± 0.0001	5.2475 ± 0.0000	1.0029 ± 0.0000	0.9817 ± 0.0000	0.030 ± 0.0000
		0.1412	3.3687 ± 0.0011	−1.8354 ± 0.0012	5.2041 ± 0.0005	1.0082 ± 0.0001	0.9402 ± 0.0006	0.0058 ± 0.0002
		0.2188	7.8977 ± 0.0056	2.8088 ± 0.0040	5.0889 ± 0.0021	1.0121 ± 0.0010	0.9000 ± 0.0010	0.0166 ± 0.0002
		0.3019	14.7550 ± 0.0128	9.8412 ± 0.0114	4.9138 ± 0.0085	1.0162 ± 0.0027	0.8777 ± 0.0075	0.0364 ± 0.0019
		0.3915	22.9307 ± 0.0627	18.2530 ± 0.0535	4.6777 ± 0.0461	1.0335 ± 0.0072	0.9842 ± 0.0425	0.2353 ± 0.0280
	RAND	0.0685	0.8277 ± 0.0010	−4.4204 ± 0.0010	5.2481 ± 0.0003	1.0024 ± 0.0024	0.9814 ± 0.0033	0.0030 ± 0.0000
		0.1412	3.3699 ± 0.0053	−1.8348 ± 0.0059	5.2047 ± 0.0016	1.0082 ± 0.0023	0.9403 ± 0.0140	0.0060 ± 0.0003
		0.2188	7.9016 ± 0.0130	2.8112 ± 0.0154	5.0904 ± 0.0100	1.0121 ± 0.0021	0.9005 ± 0.0097	0.0167 ± 0.0012
		0.3019	14.7335 ± 0.0280	9.8302 ± 0.0190	4.9033 ± 0.0180	1.0179 ± 0.0047	0.8753 ± 0.0064	0.0367 ± 0.0026
		0.3915	22.9307 ± 0.1675	18.3318 ± 0.0771	4.5989 ± 0.0962	1.0348 ± 0.0142	0.9983 ± 0.0440	0.2505 ± 0.0353

atoms in the first coordination sphere as the volume mismatch increases, and to describe the tendencies of cations of different size to cluster in the second coordination sphere. In contrast the standard deviations reported using 45 randomly chosen configurations are, as already mentioned, too large to describe these effects. The optimisations of all 35 960 possible initial configurations for a solid solution of CaO and MgO with composition $X_{MgO} = 0.125$ emphasise the success of the RDF(full) method. For the thermodynamic properties the results are within the narrow error-bar obtained using the RDF(full) method. For the structural parameters the agreement is reasonable. The RDF(full) result for γ_1 is slightly underestimated compared to that of optimising all arrangements, whereas γ_2 is too large.

Next, we compare the RDF(full) method with the random choice of initial configurations for composition $X_{HypO} = 0.5$. The standard deviations reported for both thermodynamic and structural properties when using 2656 randomly chosen configurations are small for all mismatches. Nevertheless, the standard deviations in the RDF(full) method are again significantly smaller when compared to that of a random selection of configurations for the different properties. Again, it is clear that the errors introduced because the RDF method fails to distinguish between symmetrically non-equivalent configurations with equal RDFs are very small. Note that more than 600 million configurations reduce to only 2656 RDF-non-equivalent configurations. Overall the RDF(full) method thus provides an efficient sampling-technique of configurations and reliable weightings in describing thermodynamic and structural properties at low computational cost.

We end this section with some general remarks concerning the variation of the standard deviations reported for the thermodynamic and structural properties when increasing the volume mismatch between the end members. From Table 1 we see that the standard deviation reported for the calculated thermodynamic properties of HypO and CaO solid solutions increases by several orders of magnitude when increasing the volume mismatch. The standard deviations reported for structural parameters γ_1 and γ_2 appear to be somewhat less sensitive to changes in size mismatches than the thermodynamic properties when using the random method, whereas the standard deviations reported using the RDF method appear to be strongly sensitive to an increase in the volume mismatch between the end-members being mixed.

3.3. Configurational averaging: Convergence with cell size

In Table 2 we compare the configurational averaged thermodynamic and structural properties from calculations at 1000 K using a 64-atom supercell with properties obtained using a 96-

Table 2 Calculated differences between thermodynamic and structural properties at 1000 K obtained using a 64 atom cell and results obtained using a 96 atom cell. Calculations of $\Delta H = \Delta_{mix}H$(96 atom cell) − $\Delta_{mix}H$(64 atom cell), $\Delta G = \Delta_{mix}G$(96 atom cell) − $\Delta_{mix}G$(64 atom cell), $\Delta S = \Delta_{mix}S$(96 atom cell) − $\Delta_{mix}S$(64 atom cell), $\Delta\gamma_1 = \gamma_1$(96 atom cell) − γ_1(64 atom cell), $\Delta\gamma_2 = \gamma_2$(96 atom cell) − γ_2(64 atom cell) and $\Delta V = \Delta_{mix}V$ (96 atom cell) − $\Delta_{mix}V$ (64 atom cell) are reported for a solid solution of CaO and HypO with composition $X_{HypO} = 0.125$

Volume mismatch	ΔH/kJ mol^{-1}	ΔG/kJ mol^{-1}	ΔS/J K^{-1} mol^{-1}	$\Delta\gamma_1$	$\Delta\gamma_2$	ΔV/Å^3
0.0685	−0.002	−0.002	0.000	0.004	0.007	0.000
0.1412	−0.009	−0.010	0.001	0.021	0.015	−0.001
0.2188	−0.022	−0.023	0.001	0.061	0.059	0.000
0.3019	−0.066	−0.057	−0.010	0.150	0.090	0.005
0.3915	−0.368	−0.299	−0.160	0.451	0.166	0.050

atom supercell. All optimisations are carried out in the static limit using the RDF(full) method as described previously. A solid solution of CaO and HypO with composition $X_{\mathrm{HypO}} = 0.125$ is considered.

For solid solutions of CaO and HypO where the volume mismatch is approximately 25% or less, the calculated enthalpy, entropy and Gibbs-energy differences between the two cells are less than 1%, and decreases as the volume mismatch decreases. This supports previous extensive studies on thermodynamic properties of MgO–MnO solid solutions where the thermodynamic properties obtained using a 64-atom supercell were considered sufficiently converged with respect to the cell-size.[3] In contrast, the volumes of mixing increase as much as 10% when the volume mismatch is equal to or smaller than 30%.

When the volume mismatch is large (39%) the calculated enthalpy, entropy and Gibbs energy decreases by approximately 2–4% when increasing the size of the supercell from 64 to 96 atoms. The difference between the volumes of mixing is substantial when comparing the two cells and increases as much as 20% although the absolute difference remains small. Larger cells are clearly necessary for convergence with respect to the size of the supercell for the thermodynamic properties when the volume mismatches is large (39%). We return to this later when we compare the configurational averaging and the Monte Carlo results.

The averaged number of the same type of atoms in the first and the second coordination spheres is in qualitative agreement when comparing the results obtained for the two different cells. However, quantitatively the agreement is not satisfactory. The increased clustering of similar atoms in the first coordination sphere when the size mismatch increases is more pronounced for the 96 atom super-cell. γ_1 increases by more than 20% when increasing the size of the cell. The tendency of *different* types of atoms to cluster in the second coordination sphere, appears to be influenced by the constraints imposed by periodic boundary conditions. Larger cells are needed in order to check for convergence of the structural parameters with respect to cell size.

A final remark is warranted concerning the accuracy of the RDF(full) method and the errors introduced due to cell size. Comparing the results from Table 1 and Table 2 we can see that the errors introduced because the RDF method fails to distinguish between symmetrical equivalent configurations with equal RDFs are approximately an order of magnitude smaller than those introduced due to the difference in cell size.

3.4. Configurational averaging and Monte Carlo: Variation of thermodynamic and structural properties of mixing with volume mismatch

In this section we discuss scaling of a wide range of properties using CA and MC techniques at 1000 K for solid solutions of CaO and HypO. Also, we compare in detail results obtained using Monte Carlo technique and local minima configurational averaging in order to examine cell size effects and vibrational contributions to thermodynamic and structural properties.

Optimisations and RDF(full) calculations where carried out using a 64-atom cell. The averaged properties are calculated in the static limit (using eqns. (2.1) and (2.2)) and thus measure only the configurational contribution to the property in question. Most MC calculations are carried out using a 512-atom cell (a few for comparison purposes with a 64-atom cell). The differences between results obtained using CA and MC are thus a measure of the importance of both vibrations and cell-size effects.

In Fig. 3, we plot values of $\Delta_{\mathrm{mix}}H$ as a function of the volume mismatch between the end-members for solid solution of CaO and HypO with composition $X_{\mathrm{HypO}} = 0.5$. We have also plotted enthalpy of mixing for a selection of binary oxides solid solution obtained by fitting a regular solid solution model to available enthalpy of mixing data.[12,23] The enthalpy of mixing data is insensitive to changes in the temperature.

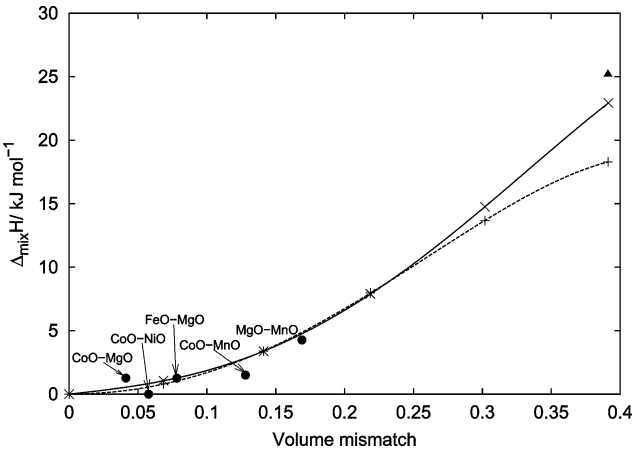

Fig. 3 $\Delta_{\mathrm{mix}}H$ *vs.* volume mismatch for solid solutions of HypO and CaO at 1000 K obtained using MC dashed line (+) and CA full line (×). The MC and CA calculations were carried out using 512- and 64-atom cells, respectively. The full triangle shows the result from a MC calculation carried out using a 64-atom cell. Full circles denote values of $\Delta_{\mathrm{mix}}H$ for a set of binary oxide solid solutions obtained by fitting a regular solid solution model to available experimental enthalpy of mixing data.[12]

When the volume mismatch is less than 30%, the agreement between MC and CA is excellent and both show that $\Delta_{\mathrm{mix}}H$ scales unambiguously quadratically with the volume mismatch between the end-members. Our results are in good agreement with available experimental data for oxide solid solutions with comparable volume mismatches, and lends support to the view that scaling of the enthalpy of mixing with the volume mismatch in these materials is mainly described by the increase of local strain due to the size mismatch between the end-members.[24]

When the volume mismatch is larger than approximately 25% there is an appreciable difference between MC values (using a 512-atom cell) and those from CA (using a 64-atom cell); $\Delta_{\mathrm{mix}}H$ continue to increase quadratically for large volume mismatches using CA, whereas the MC values show a close to linear variation. This discrepancy is mainly attributable to the difference in cell-size used in the CA and MC calculations. As discussed in a previous section $\Delta_{\mathrm{mix}}H$ decreases by approximately 2% for the largest volume mismatch (39%) when increasing the cell-size from 64 to 96 ions. This is indeed confirmed by the MC result obtained using a 64 atom cell (shown as a full triangle in Fig. 3) which is in better agreement with the CA data for the same cell size, although the latter underestimates $\Delta_{\mathrm{mix}}H$, mainly due to the neglect of vibrational contributions. Hence, for large size mismatches we find that cell size effects and vibrational contribution are important and both should be taken into account for a quantitative rather than qualitative comparison of the $\Delta_{\mathrm{mix}}H$ curves obtained from CA and MC techniques. $\Delta_{\mathrm{mix}}H$, obtained using CA and a modest size 64-atom supercell has not converged sufficiently for the present purposes for large mismatches with respect to the size of the supercell. Test calculations indicate however that the MC calculations using a 512-atom cell have converged with respect to the supercell size for all size mismatches considered here. For garnet solid solutions Bosenick *et al.*[13] have found that $\Delta_{\mathrm{mix}}H$ scaled quadratically with volume mismatch between the end-members for all mismatches studied. This trend is in agreement with our results for a different structure type since the range of volume mismatches considered in ref. 13 corresponds to volume mismatches where $\Delta_{\mathrm{mix}}H$ for solid solutions of CaO and HypO scale quadratically.

In Fig. 4 we have plotted volume of mixing *vs.* volume mismatch between the end-members for 50 : 50 samples of HypO and CaO. The sign of the volume of mixing arises essentially due to the asymmetric functional form of the

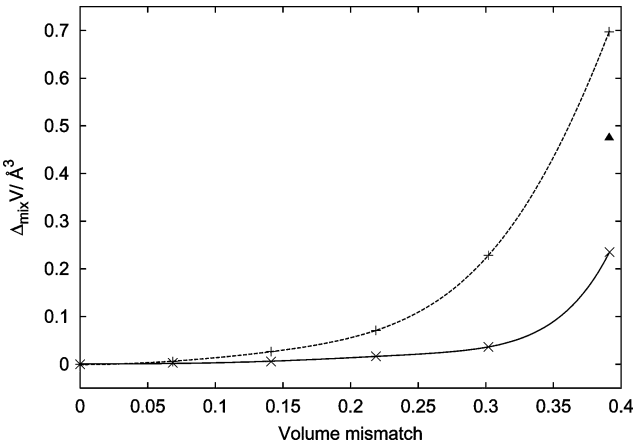

Fig. 4 $\Delta_{mix}V$ *vs.* volume mismatch between the end-members at 1000 K for a solid solution of HypO and CaO with composition $X = 0.5$. MC calculations (512 atoms) and CA calculations (64 atoms) are shown as dashed (+) and full (×) lines, respectively. The full triangle is the result from a MC calculation carried out using a 64-atom cell.

potentials. It is easier to reduce strain in the solid solution by increasing the shorter Hyp–O distance than decreasing the longer Ca–O distance; this is confirmed by examining the bond lengths in the solid solution compared with those in the end members. Test calculations carried out using MC on the 50 : 50 MgO–CaO mixture at 700 K indicate that the mean Mg–O distances increase on the average by 0.052 Å from that in bulk MgO, whereas the mean Ca–O distance decreases by 0.017 Å.

Both MC (512-atom cell) and CA (64-atom cell) calculations indicate that $\Delta_{mix}V$ increases with increasing size mismatch and scales roughly quadratically with the volume mismatch. This is in agreement with calculations of $\Delta_{mix}V$ in garnet solid solutions.[13] Although the same general trend is observed in both MC and CA results, there is a substantial difference between the two sets of results for other than small mismatches. We have already seen in section 3.3 that convergence of $\Delta_{mix}V$ with cell size is slow. To investigate this further we have also carried out a MC calculation using a 64-atom cell for the largest size mismatch, marked as a triangle in Fig. 4. This result lies closer to the CA value (also for 64-atoms) than the 512-atom Monte Carlo value. The remaining significant difference between the 64-atom MC and CA results shows the importance of including vibrations. Thus, for large size mismatches, vibrational effects as well as cell-size effects are appreciable, and conclusions based on either small cells or excluding vibrational effects need to be treated with caution. It is worth stressing that $\Delta_{mix}V$ is a small quantity and that the *absolute* differences between the results obtained using MC and CA remain small.

In Fig. 5 we have plotted excess entropies, $\Delta_{exc}S$ (rather than entropies of mixing) *vs.* volume mismatch between the end-members for a 50 : 50 sample of HypO and CaO using CA and MC techniques. We stress that our CA calculations are carried out in the static limit *i.e.*, we ignore vibrations, so the entropy calculated using CA is a measure of the configurational entropy only. The excess configurational entropy is always negative reflecting the tendency for the ions to cluster together and scales roughly quadratically with volume mismatch between the end members.

The MC calculations use the semi-grand-canonical ensemble to calculate the required chemical potential differences and thus the total entropy including both configurational and vibrational contributions.[9] The difference between the MC and the CA calculations thus allow us to estimate the contribution from the vibrational entropy of mixing. The calorimetric vibrational (non-configurational) entropy for solid solution of CoO and MgO with composition $X_{CoO} = 0.5$[23] is shown as a full circle in Fig. 5. Our estimate of the vibrational contribution to the excess entropy for the corresponding volume mismatch obtained by subtracting the CA value from the MC value is approximately 0.05 J K^{-1} mol^{-1}, which is within the experimental error bar shown in Fig. 5.[23]

The total excess entropies of mixing are positive for small mismatches and reach a maximum at approximately 25% volume mismatch (1000 K). This is consistent with a larger elongation of the Hyp–O bonds than contraction of the Ca–O bonds in the solid solution. For larger mismatches the excess entropy decreases abruptly and eventually becomes negative. For these mismatches the MC calculations (all at 1000 K) are well below the calculated critical temperatures for the solid solutions. There is strong clustering and the configurational entropy decreases. Consistent with this argument, if the Monte Carlo calculations are carried out at a larger temperature the maximum in the excess entropy moves to larger size mismatches. Overall at 1000 K for size mismatches below 32% the total excess entropy of mixing is positive although the configurational contribution is negative. Note in particular that the non-configurational contribution to the excess entropy can exceed the configurational contribution in magnitude and be opposite in sign.

The variation of γ_1 as a function of volume mismatch is plotted in Fig. 6 using CA. As discussed earlier γ_1 is strongly sensitive to small changes in the thresholds chosen for the coordination-spheres when $X_{HypO} = 0.5$, and we have rather used the results for γ_1 obtained for solid solutions of HypO and

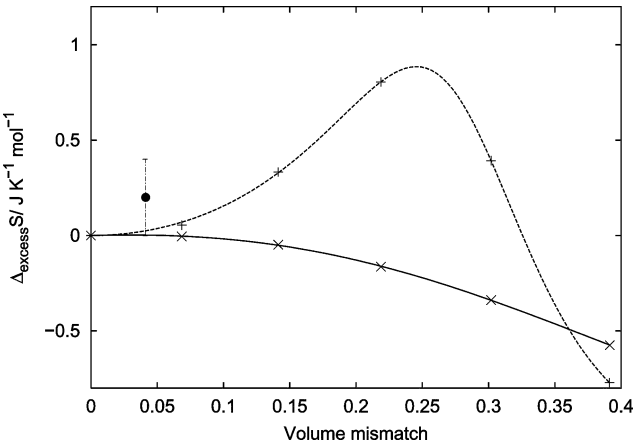

Fig. 5 Excess entropy *vs.* volume mismatch between the end-members at 1000 K for solid solutions of HypO and CaO with composition $X_{Hyp} = 0.5$. MC calculations (512 atoms) and CA calculations (64 atoms) are shown as dashed (+) and full (×) lines, respectively. The non-configurational excess entropy for solid solution of CoO and MgO with composition $X_{CoO} = 0.5$[23] is shown as a full symbol. The error bar is two standard deviations.

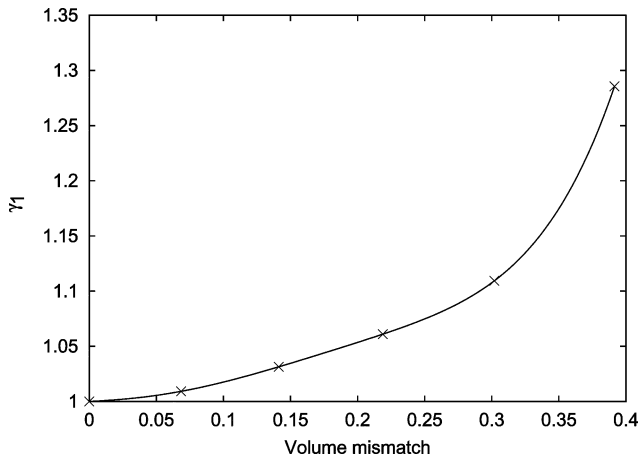

Fig. 6 γ_1 *vs.* volume mismatch between the end-members at 1000 K for solid solutions of HypO and CaO with composition $X_{HypO} = 0.125$. Calculations were carried out using CA and a 64 atom cell.

CaO with composition $X_{HypO} = 0.125$. The tendencies of equally sized atoms to cluster for all volume mismatches is evident from the figure. γ_1 increases when increasing the volume mismatch. The tendency of equally sized atoms to cluster together in the first coordination shell reflects that clustering reduces the total strain.

4. Conclusions

We have studied scaling of thermodynamic and structural properties for binary oxide solid solutions with the NaCl-type structure using configurational averaging and Monte Carlo techniques. The maximum volume mismatch studied corresponds to that in the CaO–MgO solid solution, a prototype example of a strongly non-ideal system with large miscibility gap, and a severe test of our methods.

In the present paper, we have carried out calculations using atomistic-simulation techniques. An advantage of using pair potentials is that one can mix potentials for real systems to construct potentials representing *new* hypothetical systems which allow us not only to study systematically size mismatch effects, but also to examine in detail the CA and MC techniques. Three different schemes for constructing hypothetical potentials where tested by combining the potentials for the pure binary oxides CaO and MgO. A linear interpolation technique gave enthalpies of mixing in good agreement with those for which experimental data are available.

We have shown that calculations of RDFs for all possible distributions using a 64-atom cell efficiently reduces the computational cost compared to (commonly used) techniques where all optimised configurations are chosen at random. For all but the largest size mismatches a set of RDF equivalent configurations is shown to yield very similar minimised energies and consequently the CA technique using the RDF method for configuration selection is particularly efficient. Billions of RDFs can be calculated in a few CPU hours on modern massively parallel computers. Thus configurational averaging techniques provide an efficient route for studying disordered systems, and are often computationally less expensive than Monte Carlo methods.

The enthalpies of mixing obtained using a modest sized cell and configurational averaging in conjunction with the RDF method are in good agreement with results obtained using Monte Carlo techniques for all but the largest size mismatches. When the size mismatch is large the 64-atom cell used in the configurational averaging is too small, and vibrational effects should also be taken into account in order to allow for a quantitative rather than qualitative comparison with Monte Carlo results.

Both the enthalpies and volumes of mixing are positive and scale roughly quadratically for all but the largest volume mismatches, and lends support to the view that the scaling with volume mismatch of various thermodynamic properties of mixing for these materials is explained by the increase of local strain due to the volume mismatch between the end members. Similar trends are in agreement with results obtained from calculations on garnet solid solutions where both the enthalpy and volume of mixing were shown to scale quadratically. It is important though to note that in the NaCl-type oxides the largest size mismatches may scale rather differently; the enthalpy of mixing, for example, scales roughly linearly for volume mismatches in excess of approximately 25%.

The excess entropies calculated using MC are positive and scale quadratically for small and modest size mismatches. In contrast, the CA-results, which only measure the configurational contribution to the excess entropy were negative for all mismatches.

The introduction of γ_1 and γ_2 allows us to obtain some insight into the nature of the clustering. The average number of equally sized ions in the first coordination shell was found to be larger than the ideal value for all volume mismatches, indicating that equally sized ions cluster in the first coordination shell.

The configurational averaging and Monte Carlo techniques each have their own strength and advantages which in combination, provide a powerful route for describing disordered materials. Monte Carlo is particularly useful in that vibrational effects are readily included. Configurational averaging utilising the RDF method is an effiecent technique since kinetic barriers and critical slowing downs suffered by MC are efficiently handled by CA due to its intrinsically parallelisable nature. Cases where only a few of the total number of local energy minima are thermally accessible, such as strongly non-ideal systems and, in general, disordered materials at low temperature are particularly challenging and depend critically on techniques that are able to describe adequately the lower part of the energy landscape. Here genetic algorithms can provide a useful tool.[25] Further work is in progress to develop methods using configurational averaging techniques for describing more complicated systems, such as complex minerals and grossly non-stoichiometric oxides.

Acknowledgements

This work was funded by Norges Forskningsråd (project number 14995/432). Computational facilities were made available through a grant of computing time for the Programme of Supercomputing, Norway. NLA and MYL acknowledge financial support from EPSRC which has allowed them to take part in this work and provided computational facilities for the Monte Carlo calculations.

References

1 N. L. Allan, G. D. Barrera, M. Y. Lavrentiev, I. T. Todorov and J. A. Purton, *J. Mater. Chem.*, 2000, **11**, 63.
2 N. L. Allan, G. D. Barrera, R. M. Fracchia, M. Y. Lavrentiev, M. B. Taylor, I. T. Todorov and J. A. Purton, *Phys. Rev. B*, 2001, **63**, 94203.
3 I. T. Todorov, N. L. Allan, M. Y. Lavrentiev, C. L. Freeman, C. E. Mohn and J. A. Purton, *J. Phys.: Condens. Matter.*, 2004, **16**, 2751.
4 M. Königstein, F. Cora and C. R. A. Catlow, *J. Solid State Chem.*, 1998, **137**, 261.
5 B. J. Wood, R. T. Hackler and D. P. Dobson, *Contrib. Mineral. Petrol.*, 1994, **115**, 438.
6 M. O. Zacate and R. W. Grimes, *Philos. Mag. A*, 1999, **80**, 797.
7 M. O. Zacate and R. W. Grimes, *J. Phys. Chem. Solids*, 2000, **63**, 675.
8 S. V. Stolbov and R. E. Cohen, *Phys. Rev. B*, 2002, **65**, 92203.
9 M. Y. Lavrentiev, N. L. Allan, G. D. Barrera and J. A. Purton, *J. Phys. Chem. B*, 2001, **105**, 3594.
10 P. D. Tepesch, A. F. Kohan, G. D. Garbulsky, G. Ceder, C. Coley, H. T. Stokes, L. L. Boyer, M. J. Mehl, B. P. Burton, K. Cho and J. Joannopoulos, *J. Am. Ceram. Soc.*, 1996, **79**, 2033.
11 R. C. Doman, J. B. Barr, R. N. McNally and A. M. Alper, *J. Amer. Ceram. Soc.*, 1964, **46**, 313.
12 P. K. Davies and A. Navrotsky, *J. Solid State Chem.*, 1983, **46**, 1.
13 A. Bosenick, M. T. Dove, V. Heine and C. A. Geiger, *Phys. Chem. Minerals*, 2001, **28**, 177.
14 E. Bakken, N. L. Allan, T. H. K. Barron, C. E. Mohn, I. T. Todorov and S. Stølen, *Phys. Chem. Chem. Phys.*, 2003, **5**, 2237.
15 M. B. Taylor, G. D. Barrera, N. L. Allan and T. H. K. Barron, *Phys. Rev. B*, 1997, **56**, 14380.
16 J. Gale, *J. Chem. Soc., Faraday Trans.*, 1997, **93**, 629.
17 N. I. Metropolis, A. W. Rosenbluth, M. N. Rosenbluth, A. H. Teller and E. Teller, *J. Chem. Phys*, 1953, **21**, 1087.
18 D. Frenkel and B. Smit, *Understanding Molecular Simulation*, Academic Press, San Diego, CA and London, 2nd edn., 1999.
19 B. G. Dick and A. W. Overhauser, *Phys. Rev.*, 1958, **112**, 90.
20 R. W. Grimes, *J. Am. Ceram. Soc.*, 1994, **77**, 378.
21 G. V. Lewis and C. R. A. Catlow, *J. Phys. C.*, 1985, **18**, 1149.
22 B. Winkler and M. T. Dove, *Am. Mineral.*, 1991, **76**, 313.
23 L. Wang, A. Navrotsky, R. Stevens, B. F. Woodfield and J. Boerio-Goates, *J. Chem. Thermodyn.*, 2003, **35**, 1151.
24 H. J. Greenwood, *Geochim. Cosmochim. Acta*, 1979, **43**, 1873.
25 C. E. Mohn and S. Stølen, to be published.